molecular pharmaceutics

Article

pubs.acs.org/molecularpharmaceutics

Fluorescence-Based Transport Assays Revisited in a Human Renal Proximal Tubule Cell Line

Pedro Caetano-Pinto,[†,‡] Manoe J. Janssen,[†,‡] Linda Gijzen,[†] Laurens Verscheijden,[†] Martijn J.G. Wilmer,[†] and Rosalinde Masereeuw*[,†,‡]

[†]Department of Pharmacology and Toxicology, Radboud university medical center, Radboud Institute for Molecular Life Sciences, 6500 HB Nijmegen, The Netherlands

[‡]Division of Pharmacology, Utrecht Institute for Pharmaceutical Sciences, 3508 TB Utrecht, The Netherlands

ABSTRACT: Apical transport is key in renal function, and the activity of efflux transporters and receptor-mediated endocytosis is pivotal in this process. The conditionally immortalized proximal tubule epithelial cell line (ciPTEC) endogenously expresses these systems. Here, we used ciPTEC to investigate the activity of three major efflux transporters, viz., breast cancer resistance protein (BCRP), multidrug resistance protein 4 (MRP4), and P-glycoprotein (P-gp), as well as protein uptake through receptor-mediated endocytosis, using a fluorescence-based setup for transport assays. To this end, cells were exposed to Hoechst33342, chloromethylfluorescein-diacetate (CMFDA), and calcein-AM in the presence or absence of model inhibitors for BCRP (KO143), P-gp (PSC833), or MRPs (MK571). Overexpression cell lines MDCKII-BCRP and MDCKII-P-gp were used as positive controls, and membrane vesicles overexpressing one transporter were used to determine substrate and inhibitor specificities. Receptor-mediated endocytosis was investigated by determining the intracellular accumulation of fluorescently labeled receptor-associated protein (RAP-GST). In ciPTEC, BCRP and P-gp showed similar expressions and activities, whereas MRP4 was more abundantly expressed. Hoechst33342, GS-MF, and calcein are retained in the presence of KO143, MK571, and PSC833, showing clearly redundancy between the transporters. Noteworthy is the fact that both KO143 and MK571 can block BCRP, P-gp, and MRPs, whereas PSC833 appears to be a potent inhibitor for BCRP and P-gp but not the MRPs. Furthermore, ciPTEC accumulates RAP-GST in intracellular vesicles in a dose- and time-dependent manner, which was reduced in megalin-deficient cells. In conclusion, fluorescent-probe-based assays are fast and reproducible in determining apical transport mechanisms, *in vitro*. We demonstrate that typical substrates and inhibitors are not specific for the designated transporters, reflecting the complex interactions that can take place *in vivo*. The set of tools we describe are also compatible with innovative kidney culture models and allows studying transport mechanisms that are central to drug absorption, disposition, and detoxification.

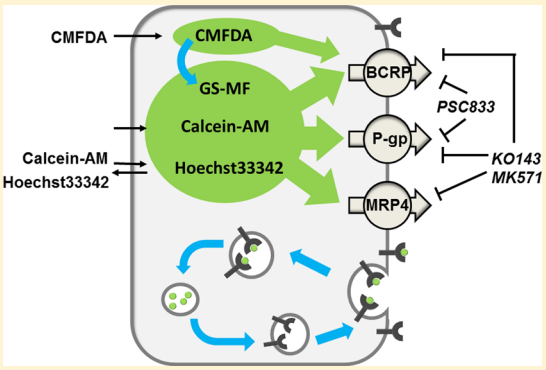

KEYWORDS: *ABC membrane transporters, receptor-mediated endocytosis, human proximal tubule cells, advanced in vitro models, fluorescence functional assays*

INTRODUCTION

Kidney proximal tubular epithelial cells (PTEC) play an active role in transporting xenobiotics, including drugs and their metabolic waste products, from the blood into the urine. In addition, PTEC are essential in reabsorbing hormones, proteins, nutrients, electrolytes, and drugs from the glomerular filtrate. These processes result in exposure of the PTEC to many potentially harmful compounds, making them an easy target for drug-related toxicity. Energy-dependent efflux across kidney tubular apical membrane, mediated by members of the ABC (ATP-binding cassette) transporter family, is a key mechanism in the renal clearance and extensively contributes to this tissue's secretory function.[1,2] The four major types of ABC efflux transporters responsible for urinary excretion are P-glycoprotein (P-gp or *ABCB1*), multidrug resistance proteins 2 and 4 (MRP2 and MRP4; *ABCC2/4*), and breast cancer resistance protein (BCRP or *ABCG2*).[2] Together, these polyspecific transporters eliminate a great variety of xenobiotics.[3,4] The substrates can be neutral, anionic, or cationic by nature, or anionic after being conjugated to glutathione, glucuronic acid, or sulfate. Although there is a significant substrate overlap between the transporters, their binding properties allow for different substrate specificities. BCRP and MRPs have a high affinity for conjugated substrates, whereas P-gp is extensively described to handle unconjugated as well as cationic xenobiotics.[5,6] During renal excretion, xenobiotics can also accumulate in proximal tubules and, over time, contribute to nephrotoxicity.[7] Furthermore, interferences with

Received: October 30, 2015
Revised: February 5, 2016
Accepted: February 12, 2016
Published: February 12, 2016

DOI: 10.1021/acs.molpharmaceut.5b00821
Mol. Pharmaceutics 2016, 13, 933−944

renal excretion can also lead to accumulation in the systemic circulation, subsequently giving rise to other adverse effects.[8]

In addition to active secretion, PTEC efficiently reabsorbs compounds from the glomerular filtrate, recovering low molelcular weight proteins and important nutrients, vitamins, and hormones bound to carrier proteins.[9,10] These compounds bind with high affinity to megalin complexes on the apical membrane of the PTEC and are internalized through receptor-mediated endocytosis. Interference with megalin-mediated endocytosis consequently leads to systemic loss of nutrients and vitamins as well as increased levels of protein in the urine. Urinary proteins directly contribute to chronic tubulointerstitial damage by inducing proinflammatory and profibrotic processes, ultimately resulting in progressive renal damage.[11,12] It is therefore important to determine which compounds affect PTEC function and protein reabsorption.

Information on ABC transporter function was largely retrieved from overexpression cell models or vesicles derived from such cell lines.[13−15] However, in these models, only one or a few individual transporter(s) can be expressed, which is far from the physiological situation.[16−18] Moreover, regulatory pathways toward the transporters either cannot be investigated or can be investigated only partially. In addition, the megalin transport mechanism has been studied mainly in nonhuman-derived cells, such as opossum kidney (OK) and the rat yolk sac cells (BN16).[19,20] To overcome these limitations, the conditionally immortalized human proximal tubule cell line (ciPTEC) has proven to be a valuable *in vitro* tool to study several pharmacological aspects of renal clearance.[21−24] Endogenous expression of the ABC efflux pumps and the endocytosis machinery, together with relevant metabolic enzymes, allows for an integrated approach on studying the effect of compounds on PTEC function. A popular strategy to evaluate xenobiotic handling in *in vitro* systems relies on fluorescent probes that are substrates for certain transporters or precursors that acquire fluorescence by metabolic activity.[25,26] Previous studies have shown that Hoechst33342 can be used to study the activity of BCRP and P-gp, whereas calcein-AM is widely used to assess P-gp function. Furthermore, we and others previously demonstrated 5-chloromethylfluorescein-diacetate (CMFDA) to become an MRP's substrate after hydrolysis and glutathione conjugation.[27,28] These compounds have in common that they can easily pass the plasma membrane by diffusion. When combining these substrates with efflux modulators, either competitors or noncompetitive inhibitors, the intracellular fluorescence increases due to substrate retention.[29] This accumulation can be measured and correlated to transport activity. In the case of endocytosis, receptor-associated protein (RAP) is efficiently bound to megalin and internalized as a complex, which is then quantified and used to evaluate defects in protein reabsorption *in vitro*.[30,31]

The aim of the present work was to investigate whether apical transport systems simultaneously active in renal proximal tubule cells can be studied using fluorescent probes and putative inhibitors.

MATERIALS AND METHODS

Chemicals. All chemicals were obtained from Sigma (Zwijndrecht, The Netherlands) unless stated otherwise. [6, 7′-^{3}H (*n*)]-Estradiol 17 β-D-glucuronide ([^{3}H]- $H_2$17βD-G) and [6′, 7′-^{3}H (*n*)]-estrone-sulfate ammonium salt ([^{3}H]-E1S) were obtained from PerkinElmer (Groningen, The Netherlands). Stock solutions of all compounds used for transport assays were prepared according to specification in either dimethyl sulfoxide (DMSO) or dH_2O. RAP-GST was kindly provided by De Matteis (TIGEM, Napels, Italy) and produced and purified as described previously.[32]

Cell Lines and Cell Culture. The ciPTEC line was derived from a healthy donor, as described previously,[23,33] and the megalin-deficient ciPTEC from a Dent's disease patient (with CLC-5 mutation c.del132−241 resulting in low-molecular-weight proteinuria, hypercalciuria, nephrolithiasis, and renal failure) was kindly provided by Prof. R. Thakker, University of Oxford, U.K.[24] Cells were cultured in phenol-red-free DMEM/F12 (Invitrogen, Breda, The Netherlands) supplemented with 10% (v/v) FCS (MP Biomedicals, Uden, The Netherlands), containing insulin (5 μg/mL), transferrin (5 μg/mL), selenium (5 ng/mL), hydrocortisone (36 ng/mL), epithelial growth factor (10 ng/mL), and tri-iodothyronine (40 pg/mL), without penicillin/streptomycin (pen/strep). ciPTEC assays were performed with cells seeded at a density of 48 000 cells per cm^2 in 96 well plates (Costar 3614, Corning, NY, U.S.A.) cultured for 24 h at 33 °C and matured for 7 days at 37 °C. Cells were subcultured at a dilution of 1:3 to 1:6 at 33 °C and experiments performed between passages 30 and 40. The Madin-Darby canine kidney (MDCKII) cells stably overexpressing BCRP or P-gp,[34,35] were kindly provided by Dr. A. Schinkel (Netherlands Cancer Institute, Amsterdam, The Netherlands) and Dr. M. Gottesman (Laboratory of Cell Biology, National Cancer Institute, U.S.A.), respectively. MDCKII cells were cultured in DMEM (Invitrogen, Breda, The Netherlands) supplemented with 10% (v/v) FCS (MP Biomedicals, Uden, The Netherlands) and 1% pen/strep, 5 units/ml (v/v). MDCK II assays were performed with cells seeded at a density of 30 000 cells per cm^2 and cultured until confluence at 37 °C. All MDCK cells lines were subcultured at a dilution of 1:3 at 37 °C in a 5% CO_2 atmosphere.

Fluorescent-Based Functional Assays in a 96-Well Plate Setup. The functional activity of BCRP, MRP4, and P-gp in ciPTEC, MDCKII-BCRP, or MDCKII-P-gp cells was evaluated using fluorescent substrates that accumulate intracellularly upon inhibition of the efflux transporters. Hoechst33342, calcein-AM (Life Technologies, Carlsbad, CA, U.S.A.) and CMFDA (Life Technologies, Carlsbad, CA, U.S.A.) were used to evaluate transporter activity. The inhibitors KO143, MK571, and PSC833 (purchased from Tocris, Bristol, U.K.) were used as typical inhibitors for BCRP, MRP4, and P-gp, respectively. A 2-fold dilution range was made for the different inhibitors starting at concentrations of 15 μM for KO143, 50 μM for MK571 and 6 μM for PSC833. To test for Hoechst retention, the cells were incubated with 1.25 μM Hoechst in combination with a gradient of each of the inhibitors for 30 min at 37 °C. Subsequently, cells were washed with ice-cold Krebs-Henseleit buffer, and fluorescence was measured immediately after (appropriate filter settings; wavelengths: excitation at 350 nm; emission at 460 nm). To determine GS-MF retention, the cells were incubated with 1.25 μM CMFDA in combination with a gradient of each of the inhibitors for 30 min, washed, and kept for an additional 30 min at 37 °C before fluorescence was measured (appropriate filter settings; wavelengths: excitation at 492 nm; emission at 517 nm). Calcein retention was assessed by incubating the cells with 1 μM calcein-AM for 60 min in combination with a gradient of each of the inhibitors. Afterward, cells were washed with cold buffer and lysed with a solution of 1% Triton X100, kept at 37 °C for an additional 60 min before fluorescence was measured (appropriate filter settings wave-

DOI: 10.1021/acs.molpharmaceut.5b00821
Mol. Pharmaceutics 2016, 13, 933−944

lengths: excitation of 485 nm; emission of 530 nm). Each solution was prepared in buffer at pH of 7.4, and fluorescence readings were performed using a Victor X3Multilabel plate reader (PerkinElmer, Waltham, U.S.A.). All experiments were performed in a 96-well plate setup in triplo with a minimum of three separate experiments.

Fluorescence-Based, Receptor-Mediated Endocytosis Assay. Endocytosis was evaluated by RAP-GST uptake over time and at different concentrations in ciPTEC cultured in 96-well black chimney plates (Costar 3690, Corning, NY, U.S.A.). Cells were incubated with RAP-GST at a 3-fold dilution range (starting at 7.5 μg/mL) for 2 h, or with one concentration of RAP-GST (2.5 μg/mL) for different times (1 or 6 h) and on ice. To compare the uptake between normal ciPTEC and megalin-deficient ciPTEC, cells were incubated for 1 h with RAP-GST (2.5 μg/mL). After incubation, cells were fixed in 4% PFA/PBS for 15 min, washed with PBS, and permeabilized for 10 min with 0.1% Triton/PBS. Next, samples were incubated overnight at 4 °C with anti-GST antibody (GE Healthcare 27457701, Goat polyclonal, 1:1600 in 1%BSA/PBS), washed three times with PBS, and incubated for 2 h at room temperature with fluorescently labeled secondary antibody (Molecular probes A11055, Donkey anti goat, Alexa Fluor 488, 1:500 in 1%BSA/PBS). Finally, samples were washed three times with PBS and fluorescence was recorded with the Victor X3Multilabel plate reader.

Cytoplasmic Enzyme Activity. Enzymatic activity required to form fluorescent products from calcein-AM and CMFDA was evaluated by exposing cell lysates of the cell lines to the same concentration of fluorescent substrates used in the functional assays (viz., Hoechst33342 at 1.25 μM, CMFDA at 1.25 μM and calcein-AM at 1 μM). Cell lysates were obtained from matured ciPTEC and MDCKII cells by exposing cell suspensions (80 000 cells per 100 μL) to heat shock, first immersing the cells in liquid nitrogen until completely frozen and subsequent immersion in heated tap water. This procedure was repeated three times. Afterward, the suspensions were centrifuged for 15 min at 10 000 rpm, and the supernatant collected and stored at −80 °C. The assay was performed in 96-well black chimney plates after addition of 50 μL of cell lysates followed by 50 μL of each of the fluorescent substrates. Fluorescence was monitored over time for 90 min at 37 °C, with measurements performed every 2 min using a Victor X3Multilabel plate reader.

Confocal Microscopy. To visualize the uptake of fluorescent substrates and their accumulation, matured ciPTEC, cultured in a Lab-TeK8 chambers slide (Thermo Scientific, Waltham, MA, U.S.A.), were incubated with the substrates Hoechst33342 (1.25 μM) combined with KO143 (10 μM), CMFDA (1.25 μM) combined with MK571 (10 μM) and calcein-AM (1 μM) combined with PSC833 (5 μM) for 30 min. Images were acquired via an CV7000S high-content imager (Yokogawa, Tokio, Japan). For microscopic evaluation of receptor-mediated endocytosis, cells were cultured on a 8-well chambered coverslip (Ibidi 80826, Planegg-Martinsried, Germany), incubated for 1 h with RAP-GST (2.5 μg/mL) before fixation, permeabilization and fluorescent labeling with an Alexa 488 labeled antibody (see also receptor mediated endocytosis assay). After nuclear stain (DAPI; 300 ng/mL) images were acquired via an Olympus FV1000 confocal microscope (Zoeterwoude, The Netherlands

MRP4 and BCRP Membrane Vesicle Uptake Transport Inhibition Assay. Substrate and inhibitor specificity was investigated further using the membrane vesicle uptake assays, as established in our laboratory.[36−38] Crude membrane vesicles were isolated from Human Embryonic Kidney (HEK) 293 cells, a widely used, nonpolarized permissive cell line, that express the transfected transporters in both the plasma membrane and intracellular vesicles.[39,40] The uptake of radiolabeled substrates [^{3}H]-$H_2$17βG and [^{3}H]-E1S by MRP4 and BCRP vesicles was analyzed as described previously.[15,36,41] Briefly, the vesicles (PharmTox; Nijmegen, The Netherlands, http://www.pharmtox.nl) were prepared by cloning MRP4, BCRP, or enhanced yellow fluorescent protein (eYFP) as control behind a CMV promotor into a Baculovirus that was used to transduce HEK293 cells. Cell membranes were isolated (100000 g fraction) and resuspended in ice-cold isotonic TS buffer (10 mM Tris-HEPES and 250 mM sucrose, pH 7.4), followed by high shear passage (100 μm opening) to prepare membrane vesicles. Vesicles were snap-frozen in liquid nitrogen and stored at −80 °C until further processing. For the uptake assays, 25 μL of Tris-Sucrose (TS) buffer containing 4 mM ATP, 10 mM $MgCl_2$ and radiolabeled substrate was added to 5 μL of membrane vesicles (1.5 mg/mL). The transport assay was performed in the presence of the highest concentrations of inhibitors and substrates used in the 96-well plate assays described: KO143 (15 μM), MK571 (50 μM), PSC833 (6 μM), Hoechst33342 (1.25 μM), CMFDA (1.25 μM), calcein-AM (1 μM) and DMSO (2%, vehicle). Transport was achieved by incubating the mixture at 37 °C for 1 min (BCRP vesicles) or 5 min (MRP4 vesicles), the transport was stopped by placing the samples on ice and adding 150 μL ice cold TS buffer. Afterward, the samples were transferred to a 96 well filter plate (Millipore, Etten-Leur, The Netherlands), preincubated with TS buffer and filtered using a Multiscreen HTS-Vacuum Manifold filtration device (Millipore). Subsequently, 2 mL of scintillation liquid was added to each filter, and radioactivity was measured by liquid scintillation counting. EYFP-membrane vesicles and AMP were used as negative controls, and all experiments were performed in triplicate.

Gene Expression. Transporters gene expression in matured ciPTEC and Human Kidney (acquired from healthy donors under consent) samples was performed by isolationg total using an RNeasy Mini kit (Qiagen, Venlo, The Netherlands) according to the manufacturers recommendations. Subsequently, cDNA was generated using the Omniscript RT-kit (Qiagen). Following cDNA-synthesis, quantitative PCR was performed using a CFX96 Real-Time PCR detection system (Biorad, Veenendaal, The Netherlands). GAPDH was used as housekeeping gene, and relative expression levels were calculated as fold change using the $2^{-\Delta\Delta CT}$ method. The primer-probe sets were obtained from Applied Biosystems: GAPDH - hs99999905_m1; BCRP - hs00184979_m1; MRP4 - hs00195260_m1 and Pgp - hs00184500_m1.

Pharmacokinetic and Statistical Data Analysis. Efflux activity was calculated by normalizing fluorescence intensity (upon inhibition), expressed in arbitrary units (a.u.), to baseline values (no inhibitor) after subtraction of background, prior to all calculations. As inhibition of efflux activity led to an increase in total fluorescence, the efflux activity is depicted as the inverse of the fold increase in fluorescence

$$\text{efflux activity} = \left(1 \div \left[\frac{\text{a. u.}}{\text{baseline}}\right]\right) \times 100$$

Nonlinear regression with a variable slope constraining the top to 100% was used to fit the normalized data, using GraphPad Prism 5.02 (GraphPad software, San Diego, CA, U.S.A.). Differences

DOI: 10.1021/acs.molpharmaceut.5b00821
Mol. Pharmaceutics 2016, 13, 933−944

Table 1. Efflux Transporters Relative Expression in ciPTEC and Human Kidney(HuKid)[a]

	ΔCt		$2^{-\Delta Ct}$		relative expression
	ciPTEC	HuKid	ciPTEC	HuKid	ciPTEC vs HuKid
BCRP	10.8 ± 0.7	6.7 ± 1.0	$6.5 \times 10^{-4} \pm 3.2 \times 10^{-4}$	0.01 ± 0.008	6.5%
Pgp	8.8 ± 0.4	4.5 ± 0.7	$2.3 \times 10^{-3} \pm 9.2 \times 10^{-4}$	0.05 ± 0.02	4.6%
MRP4	6.6 ± 0.6	3.9 ± 0.3	$1.1 \times 10^{-2} \pm 5.4 \times 10^{-3}$	0.07 ± 0.02	15.7%
MRP2	15.6 ± 0.2	[b]	$2.0 \times 10^{-5} \pm 2.8 \times 10^{-6}$	[b]	[b]

[a]Values are shown in mean ± standard deviation. [b]MRP2 could not be determined.

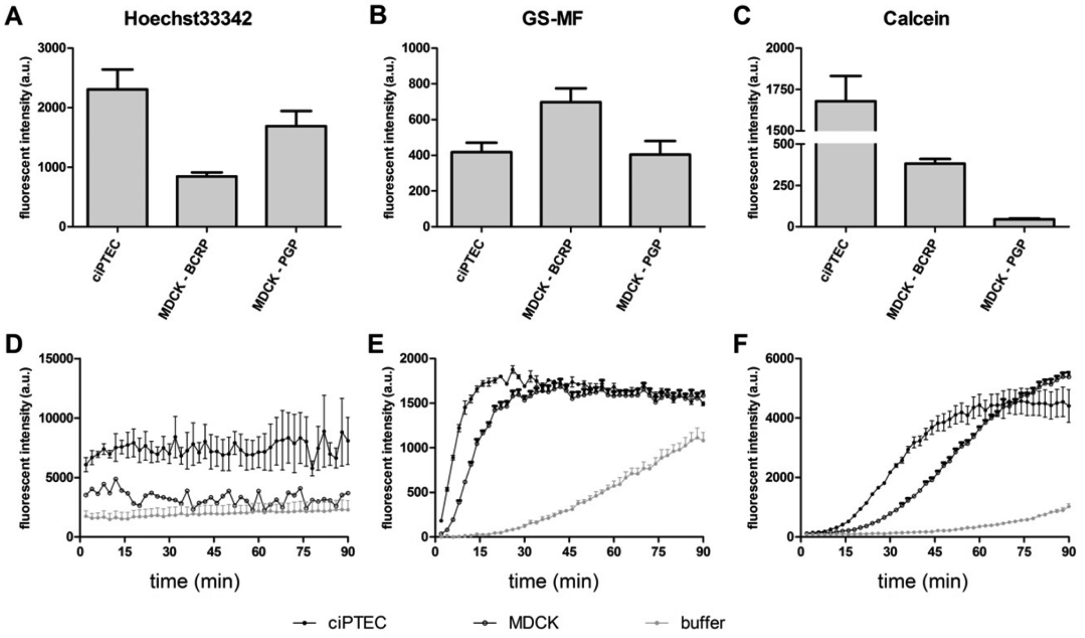

Figure 1. Differential fluorescent substrates retention and enzyme activity in ciPTEC and MDCKII cell lines. Hoechst33342 (1.25 μM) retention (A) was lower in MDCKII-BCRP and MDCKII-Pgp. CMFDA/GS-MF (1.25 μM; B) was similarly retained in ciPTEC and MDCKII-Pgp but in a lower fashion than in MDCKII-BCRP. Calcein (1 μM; C) was efficiently effluxed of MDCKII-Pgp cells while it accumulated greatly in ciPTEC. Differential substrates retention between the cell lines is indicative of the disparities in endogenous and overexpressed transport systems. By using cell lysates of both ciPTEC and MDCKII parent cell line, it was possible to determine the intracellular enzyme activity over time (90 min), in the presence of the substrates Hoechst33342 (1.25 μM; D), CMFDA (1.25 μM; E) and calcein-AM (1 μM; F).

between groups were considered to be statistically significant when $p < 0.05$ when performing a one-tailed Student's *t*-test. All data are presented as mean ± SEM of at least three separate experiments performed in triplicate, unless stated otherwise. Statistical analysis to determine differences between IC_{50} values was performed within every substrate via two-way ANOVA. Statistical significant differences were set to $p < 0.05$.

RESULTS

To study the transport activity in absence and presence of inhibitors, we compared three different cell models. The ciPTEC show many characteristics of human PTEC, including cell polarization, monolayer organization, expression of tight junction proteins, as well as transporter and metabolic enzyme activity.[18,19,23,32] We investigated the relative expression levels of the ABC transporters BCRP, P-gp, MRP2, and MRP4 in comparison to the human kidney. Table 1 shows that MRP4 is the most abundantly expressed transporter relative to BCRP and Pgp in both ciPTEC and human kidney, whereas MRP2 is only moderately expressed in ciPTEC. BCRP and Pgp show comparable expression levels.

The MDCK overexpression lines were used as positive controls for BCRP and P-gp activity. Hoechst33342 was used to evaluate BCRP activity directly, whereas calcein-AM and CMFDA gain fluorescent properties upon hydrolysis (methyl group cleavage) in the cytoplasm, and, in case of CMFDA, further conjugation to carboxyfluorescein-glutathione (GS-MF) with the replacement of the chlorine group. The fluorescent end products were used to determine P-gp (calcein) and MRP's (GS-MF) activities, respectively. The inhibitors KO143, MK571, and PSC833 were used to block BCRP, MRP4, and P-gp activity, respectively.[29,42,43] To evaluate their effect on the different cell lines, we tested the three inhibitors in combination with all three substrates.

ciPTEC and MDCKII Overexpression Cells Have Differential Fluorescent Substrate Retention. Substrate retention levels varied between the different cell lines used as an indication of the transporters activity in each cell type. MDCKII-BCRP cells showed the lowest Hoechst33342 accumulation while ciPTEC presented the highest (Figure 1A), consistent with the high expression of BCRP in the MDCKII overexpression cell line. For GS-MF, ciPTEC and MDCKII-Pgp presented similar intensities and MDCKII-BCRP the highest (Figure 1B). When incubated with calcein-AM, the highest retention was observed in ciPTEC, while MDCKII-P-gp showed minor accumulation (Figure 1C),

DOI: 10.1021/acs.molpharmaceut.5b00821
Mol. Pharmaceutics 2016, 13, 933−944

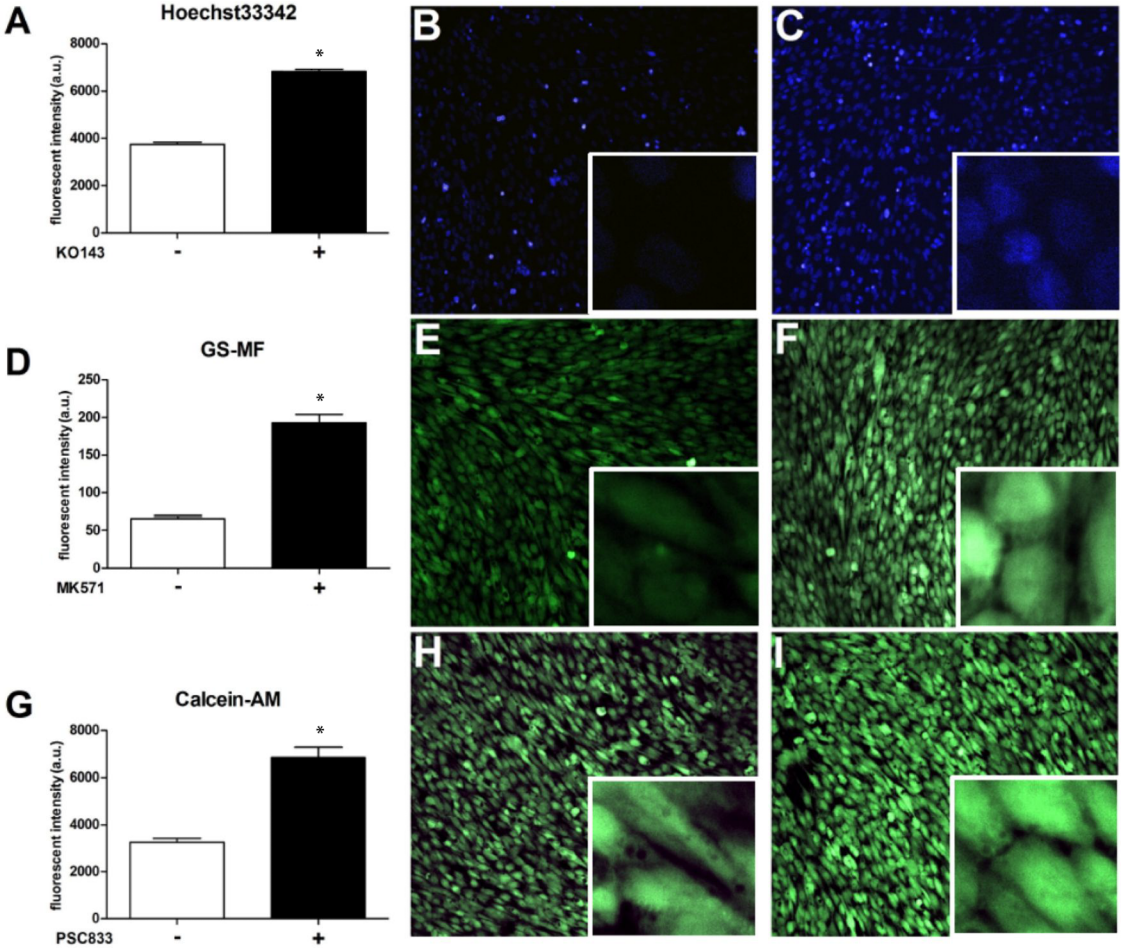

Figure 2. Fluorescent substrates accumulate in ciPTEC in the presence of efflux transport blockers. An increase in fluorescence was observed when cells were incubated with the fluorescent substrates Hoechst (1.25 μM; A), CMFDA (1.25 μM; D), Calcein-AM (1 μM; G) without inhibitors (B,E,H) or in the presence of inhibitors (C,F,I). Inhibitors promoted the intracellular accumulation of the fluorescent substrates, as depicted in the representative images and quantified in the bar graphics. Images were acquired with a 20× objective, and in the bottom right corner is presented a magnification of the same image in which only a few cells are detailed. (black bars; $n = 3$, *$p < 0.05$).

Table 2. Inhibitory Potencies of KO143, MK571, and PSC833 on Hoechst33342, GS-MF, and Calcein Efflux by ciPTEC

		IC_{50} (M)		
substrate	cell type	KO143	MK571	PSC833
Hoechst33342				
	ciPTEC	$4.4 \times 10^{-6} \pm 0.9 \times 10^{-6}$	$5.1 \times 10^{-6} \pm 0.9 \times 10^{-6}$	$1.3 \times 10^{-6} \pm 0.3 \times 10^{-6}$[e]
	MDCKII-BCRP	$3.5 \times 10^{-6} \pm 0.1 \times 10^{-6}$	$10.1 \times 10^{-6} \pm 3.7 \times 10^{-6}$[d]	$2.0 \times 10^{-6} \pm 1.1 \times 10^{-6}$[e]
	MDCKII-Pgp	$3.6 \times 10^{-6} \pm 1.5 \times 10^{-6}$	$24.2 \times 10^{-6} \pm 2.9 \times 10^{-6}$[a,b,d]	$0.9 \times 10^{-6} \pm 0.5 \times 10^{-6}$[e]
CMFDA/GS-MF				
	ciPTEC	$2.7 \times 10^{-6} \pm 0.2 \times 10^{-6}$	$6.4 \times 10^{-6} \pm 1.3 \times 10^{-6}$	$1.0 \times 10^{-6} \pm 0.2 \times 10^{-6}$
	MDCKII- BCRP	$2.3 \times 10^{-6} \pm 0.9 \times 10^{-6}$	$8.5 \times 10^{-6} \pm 2.4 \times 10^{-6}$	$1.2 \times 10^{-6} \pm 0.4 \times 10^{-6}$
	MDCKII-Pgp	$3.6 \times 10^{-6} \pm 1.7 \times 10^{-6}$	$22.2 \times 10^{-6} \pm 10.3 \times 10^{-6}$[a,b,d]	$0.7 \times 10^{-6} \pm 0.3 \times 10^{-6}$[e]
Calcein				
	ciPTEC	$2.5 \times 10^{-6} \pm 0.5$ x10^{-6}	$10.2 \times 10^{-6} \pm 3.1 \times 10^{-6}$[d]	$0.7 \times 10^{-6} \pm 0.5 \times 10^{-6}$[e]
	MDCKII- BCRP	$2.4 \times 10^{-6} \pm 0.4 \times 10^{-6}$	$9.9 \times 10^{-6} \pm 5.8 \times 10^{-6}$[d]	$1.2 \times 10^{-6} \pm 0.7 \times 10^{-6}$[e]
	MDCKII-Pgp	$1.7 \times 10^{-6} \pm 0.1 \times 10^{-6}$	$5.3 \times 10^{-6} \pm 2.3 \times 10^{-6}$	$0.8 \times 10^{-6} \pm 0.1 \times 10^{-6}$

Values are presented as mean ± SD. Statistical significant differences ($p < 0.05$) between cell types (same inhibitor) are represented by [a](ciPTEC), [b](MDCK-BCRP), [c](MDCK-Pgp). Statistical significant differences ($p < 0.05$) between inhibitors (same cell type) are represented by [d](KO143), [e](MK571), [f](PSC833).

in agreement with the overexpression of the transporter in the latter cell line.

ciPTEC and MDCKII Cells Have Similar Enzyme Activities. Since enzyme activity is required to convert CMFDA and calcein-AM into their fluorescent counterparts (GS-MF and calcein, respectively), the efficiency of this conversion was compared in cell lysates of ciPTEC and MDCKII cells. As expected, Hoechst33342 fluorescence was not

DOI: 10.1021/acs.molpharmaceut.5b00821
Mol. Pharmaceutics 2016, 13, 933−944

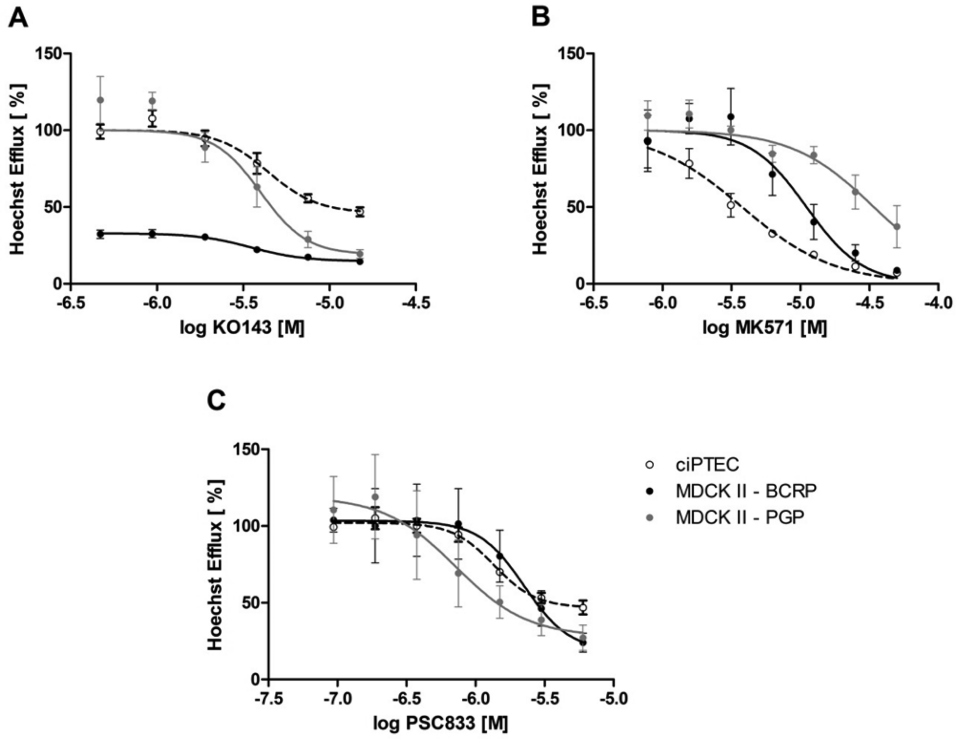

Figure 3. Dose response effects of the inhibitors KO143 (A), MK571 (B), and PSC833 (C) on Hoechst33342 retention in ciPTEC (dotted line), MDCK II-BCRP (black line), and MDCK II-Pgp (gray line). To determine IC_{50} values, nonlinear regression with variable slope constraining the top to 100% was performed using at least six concentrations of each inhibitors. Activity was considered 100% in the respective cell lines, in the absence of any inhibitor.

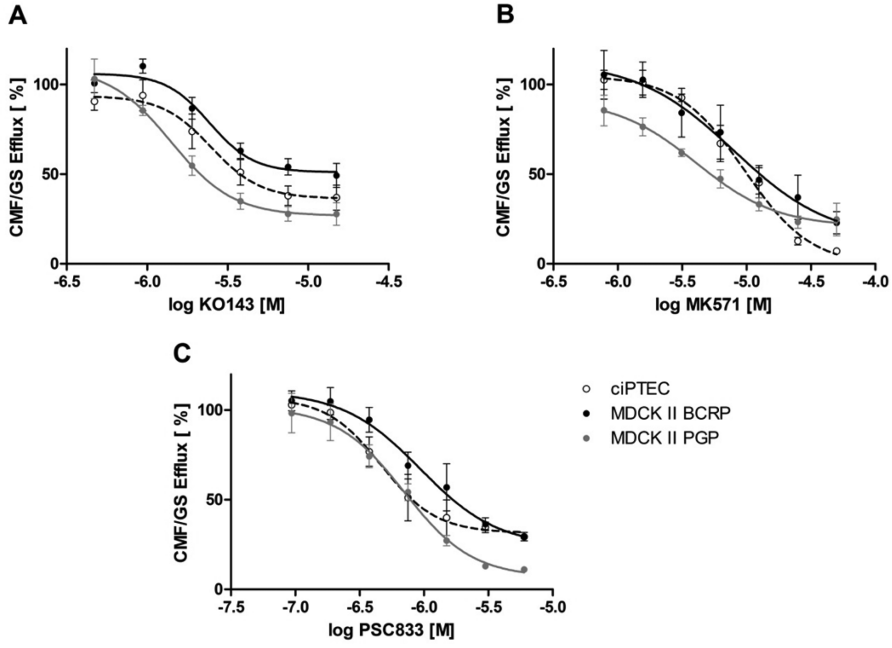

Figure 4. Dose-response effects of the inhibitors KO143 (A), MK571 (B), and PSC833 (C) on CMFDA/GS-MF retention in ciPTEC (dotted line), MDCKII-BCRP (black line), and MDCKII-Pgp (gray line). To determine IC_{50} values, nonlinear regression with variable slope constraining the top to 100% was performed using at least six concentrations of each inhibitor. Activity was considered 100% in the respective cell lines in the absence of any inhibitor.

influenced when incubated with cell lysates nor showed a time-dependent effect (Figure 1D). When cell lysates were incubated with either CMFDA (Figure 1E) or calcein-AM (Figure 1F) at 37 °C, the fluorescence behavior over time was similar in ciPTEC and MDCKII, although ciPTEC showed a more rapid initial increase in signal. Both substrates were also slowly transformed over time in buffer (without cells). The inhibitors used in the functional assays (KO143, MK571, and PSC833) did not

DOI: 10.1021/acs.molpharmaceut.5b00821
Mol. Pharmaceutics 2016, 13, 933−944

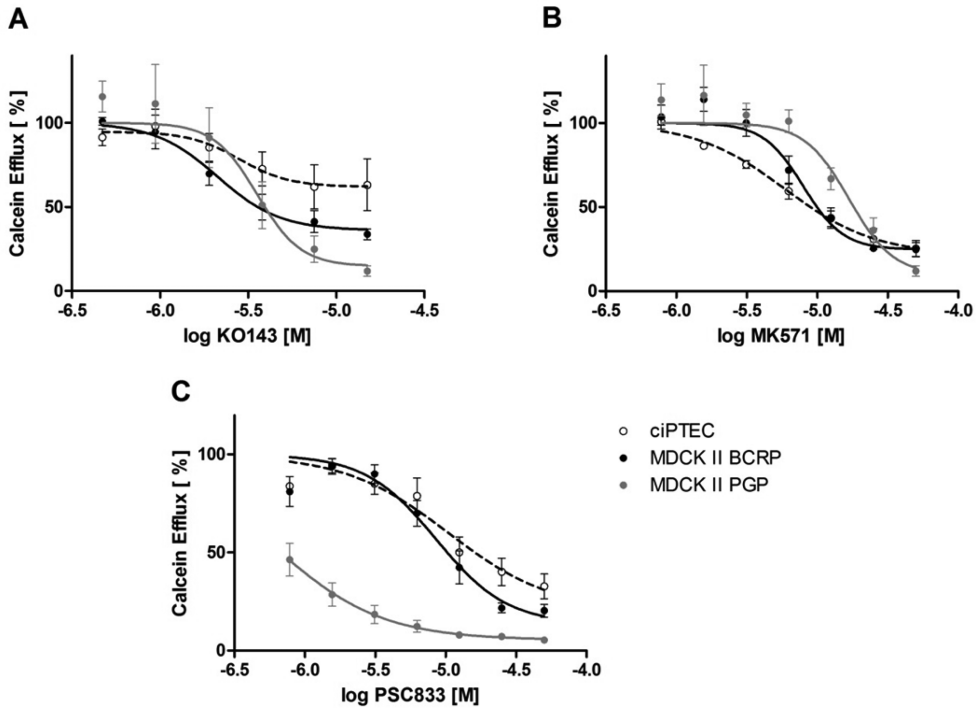

Figure 5. Dose response effects of the inhibitors KO143 (A), MK571 (B), and PSC833 (C) on calcein retention in ciPTEC (dotted line), MDCKII-BCRP (black line), and MDCKII-Pgp (gray line). To determine IC50 values, nonlinear regression with variable slope constraining the top to 100% was performed using at least six concentrations of each inhibitor. Activity was considered 100% in the respective cell lines in the absence of any inhibitor.

interfere with the enzyme activity in converting the substrates (data no shown).

Fluorescent Substrates Accumulate in ciPTEC upon Efflux Transport Inhibition. Model efflux inhibitors increased the intracellular accumulation of fluorescent substrates in ciPTEC, as demonstrated in Figure 2. In the presence of KO143, Hoechst33342 fluorescence increased 1.8-fold (Figure 2A), GS-MF retention increased 3.0-fold in the presence of MK571 (Figure 2D), and PSC833 increased calcein fluorescence 2.1-fold (Figure 2G). These results indicate that efflux can effectively be blocked in ciPTEC. The substrates' intracellular accumulations upon efflux inhibition could be confirmed with confocal microscopy. A clear nuclear accumulation was observed for Hoechst33342 (Figure 2B,C), whereas GS-MF (Figure 2E,F) and calcein (Figure 2H,I) accumulated predominantly in the cytoplasm.

Inhibitors and Substrates Used for Efflux Pumps Lack Specificity. The efflux of the model substrates Hoechst33342, GS-MF, and calcein was investigated further in a concentration-dependent manner with all combinations of inhibitors, to determine efflux activity and substrate and inhibitor specificities (Figures 3−5). Inhibition curves were analyzed by nonlinear curve fitting and a summary of the IC_{50} values obtained for all interactions is presented in Table 2.

Hoechst33342 Efflux. The prototype inhibitor for BCRP activity and Hoechst33342 retention is KO143 (Figure 3A), which reduced the efflux in MDCKII-BCRP and MDCKII-P-gp by 85 and 80% (Figure 1), respectively. In ciPTEC, efflux was reduced by 46.9 ± 5.0%, suggesting efflux is only partially BCRP mediated. On the other hand, Hoechst33342 efflux in ciPTEC could be inhibited by MK571 (Figure 3B), suggesting Hoechst33342 efflux is mediated by MRP transport as well. In presence of MK571 (Figure 3B), ciPTEC and MDCKII-BCRP presented comparable efflux inhibitions (7.1 ± 0.3% and 9 ± 2%, respectively). When exposed to the Pgp blocker PSC833, Hoechst33342 efflux was reduced to 46 ± 8% in ciPTEC, to 24 ± 11% in MDCKII-BCRP, and to 27 ± 14% in MDCKII-P-gp (Figure 3C), supporting the role of P-gp in Hoechst3342 efflux as well.

CMFDA/GS-MF Efflux. For CMFDA/GS-MF efflux inhibition KO143 showed a comparable potency (Table 2) in ciPTEC and MDCKII-BCRP, while the highest inhibition, up to 28 ± 11%, was found in MDCKII-P-gp cells (Figure 4A). MK571 (Figure 4B) promoted a considerable inhibition in all cell lines tested, with the highest decrease of efflux in ciPTEC (up to 7.0 ± 1.8%). PSC833 (Figure 4C) promoted similar maximal inhibitions in all cell lines, except for MDCKII-Pgp, which was most sensitive (11.0 ± 1.8%). The highest reduction in overall transport was found in ciPTEC. Taken together, these results underline the crossover in inhibitor specificities, pointing to a role for BCRP, P-gp, and MRP transporters in handling CMFDA and/or its derivatives.

Calcein Efflux. In MDCKII-P-gp, KO143 could inhibit calcein efflux up to 12 ± 6% (Figure 5A), whereas in ciPTEC the maximum inhibition was only 63 ± 27%. When exposed to MK571 (Figure 5B) MDCKII-BCRP and ciPTEC showed similar inhibitions in efflux; up to 25 ± 7% and 25 ± 8%, respectively. PSC833 (Figure 5C), affected calcein efflux mostly in MDCKII-P-gp cells (5.3 ± 1.6%) with the highest potency (Table 2). ciPTEC and MDCKII-BCRP presented similar IC_{50} values, whereas ciPTEC showed the lowest efflux reduction (32.7 ± 10.9%). These findings are consistent with KO143 exhibiting inhibitory properties toward P-gp and further underscores a lack of substrate and inhibitor specificity.

Fluorescent Substrates and Inhibitors Affect BCRP and MRP4 Activity in Vesicles. Membrane vesicles were used as single expression transporter systems for P-gp, BCRP, and MRP4 in order to determine the specific effects of the substrates and

DOI: 10.1021/acs.molpharmaceut.5b00821
Mol. Pharmaceutics 2016, 13, 933−944

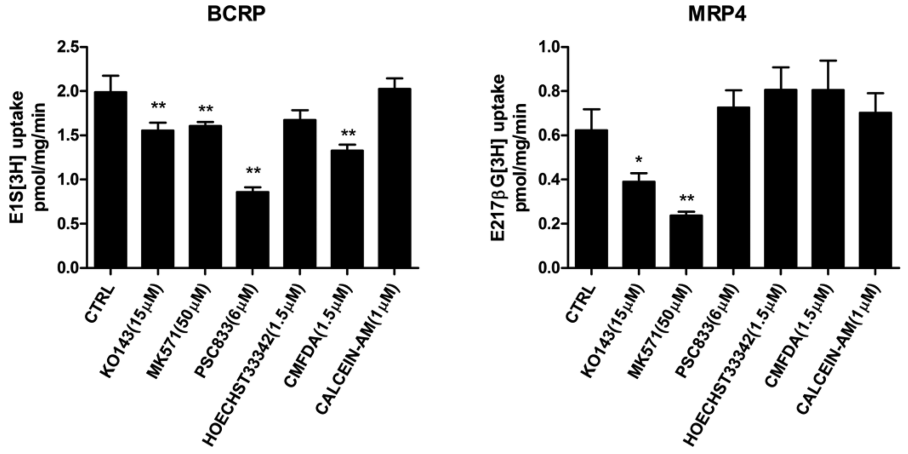

Figure 6. ATP-dependent uptake of E1S−^{3}H mediated by BCRP (A) or E217βB−^{3}H uptake mediated by MRP4 (B) was studied in HEK293-cell-derived vesicles. DMSO was used as vehicle (ctrl), along with inhibitors KO143, MK571, PSC833, and substrates Hoechst33342 and CMFDA. BCRP-mediated uptake is significantly decreased by KO143, MK571, PSC833, and CMFDA. MRP4 is affected only by KO143 and MK571. Statistical analysis was performed via unpaired Student's *t*-test. *p < 0.05 and **p < 0.01 compared to control.

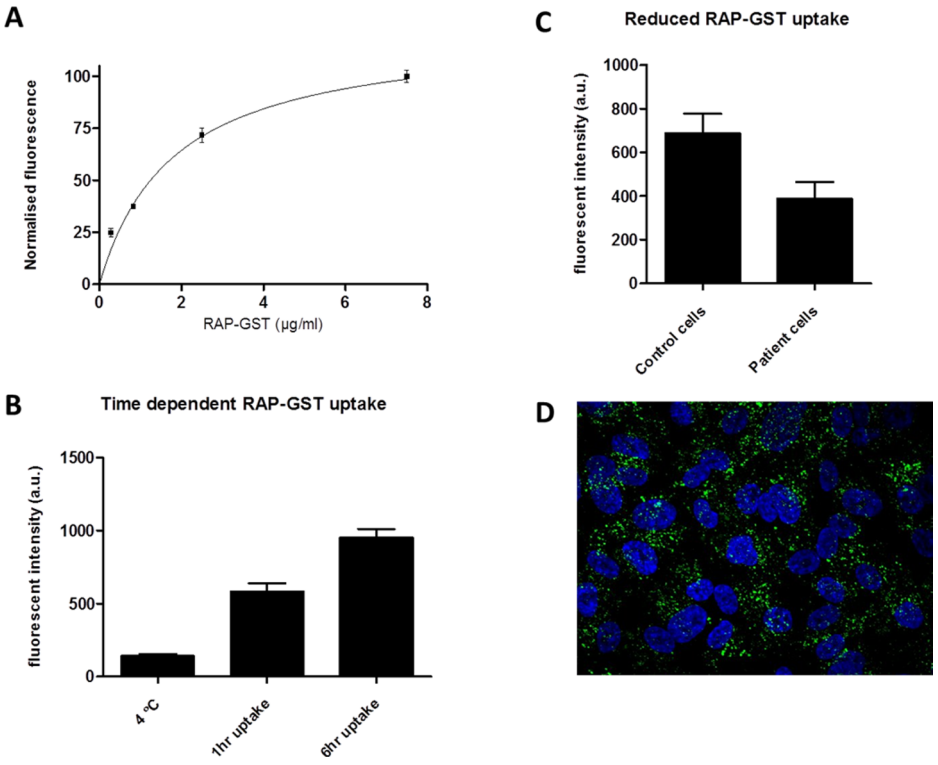

Figure 7. Endocytosis-mediated protein reabsorption in ciPTEC. Cells were incubated at 37 °C with different concentrations of RAP-GST for 2 h (A) or with 2.5 μg/mL RAP-GST for different periods of time (B). Protein surface binding was determined by incubating cells with RAP-GST on ice for 30 min (B). Protein uptake was compared between control ciPTEC cells and cells from patients with Dent's disease (C). Immunofluorescent image of fluorescently labeled RAP-GST after uptake in control ciPTEC (D).

inhibitors used. Using NMQ as a substrate,[44] it was not possible to determine the interaction between the compounds used and P-gp (data not shown). To evaluate BCRP and MRP4 activities, we used [^{3}H]-E1S and [^{3}H]-$H_2$17βG as substrates, respectively. The radioactive substrate uptake inhibition in BCRP or MRP4 vesicles is a direct indication of the potency of the compound tested. In BCRP vesicles (Figure 6A), [^{3}H]-E1S uptake was significantly reduced by KO143, MK571, PSC833, and CMFDA, compared to the control condition. On the other hand, MRP4-mediated uptake of [^{3}H]-$H_2$17βG (Figure 6B) was only significantly reduced by KO143 and MK571 compared to control.

Endocytosis-Mediated Reabsorption in ciPTEC. Protein reabsorption is another important function of proximal tubular cells and essential for renal physiology and drug safety assessments. The megalin ligand RAP-GST is efficiently taken up by ciPTEC and has been used to study the receptor-mediated endocytosis machinery in patient cells in comparison to ciPTEC from healthy controls.[30,31] The quantification is traditionally done on fluorescent microscopy images, which is a very laborious and time-consuming process. Here we optimized the staining

DOI: 10.1021/acs.molpharmaceut.5b00821
Mol. Pharmaceutics 2016, 13, 933−944

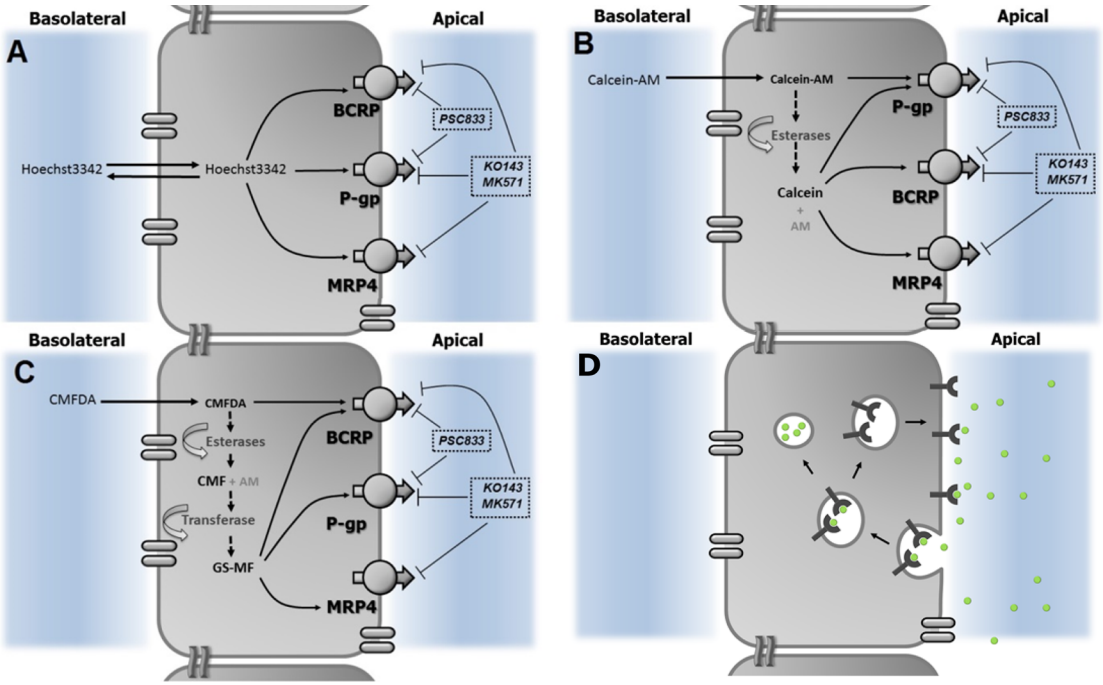

Figure 8. Graphic presentation of substrate handling, transport inhibition, and reabsorption in ciPTEC. Hoechst (A), calcein (B), and CMFDA (C) intracellular fate, and the transporters responsible for efflux are depicted in combination with the inhibitors used. RAP-GST uptake (D) through receptor-mediated endocytosis represents the protein reabsorption capacity of these cells.

and quantification for a 96-well plate format with detection in a fluorescent plate reader. We could show that RAP-GST was efficiently taken up by the cells in a time- and concentration-dependent manner (Figure 7A,B). To evaluate the initial binding of ligand to the megalin receptors on the cell (prior to internalization), we incubated the cells for 30 min on ice in the presence of ligand (Figure 7B). The binding on ice was 24% of the uptake after 1 h, suggesting that within this time frame the initial amount of receptor on the surface can be internalized and replenished on the cell surface several times. Dent's disease ciPTEC showed a RAP-GST uptake of 57% of the control cells. Furthermore, the fluorescent labeling was consistent with endocytotic vesicles and showed minor background fluorescence.

DISCUSSION

The renal proximal tubule is a versatile part of the nephron, which plays a crucial role in the active secretion and reuptake of numerous exogenous (e.g., drugs), as well as endogenous compounds. These processes are mediated by a wide variety of transport proteins, present in the basolateral and apical membranes of PTEC. In this study, we describe the application of fluorescent-based assays in a 96-well plate format to provide reproducible data on transporter activity and drug interactions on transport activities present in the proximal tubule apical membrane. We tested the efflux of several classical substrates (Hoechst33342, CMFDA/GS-MF, and calcein(-AM)) in cell models expressing different transporters simultaneously or in parallel and demonstrated that the substrates are not transported by one particular transporter, as was previously described.[45] Furthermore, we used several known inhibitors (KO143, MK571, and PSC833) for the relevant transporters and showed that these inhibitors (partially) inhibit the function of other transporters as well. We believe that our data provide insight into the complex interactions that take place *in vivo*. These interactions should be taken into account when screening for drug interactions. This may be done using a more advanced human cell model, such as ciPTEC, in which membrane transporters BCRP, P-gp, and MRP4 are simultaneously expressed. Despite positive detection by Western blotting,[23,33] the localization of these transporters via immunocytochemistry has been unsuccessful so far, given the limitations of detecting low expressing endogenous proteins in polarized cells growing in a monolayer. Furthermore, the expression and activity of organic cation transporter 2 (OCT2) was reported in ciPTEC,[22] and a broad panel of phase I and II metabolic enzymes were expressed at similar levels as in primary human proximal tubule cells, including cytochromes P450 (CYP) CYP3A4, CYP4A11, CYP2D6, UDP-glucuronosyltransferases (UGT) 1A1, UGT1A9, UGT2B7, and UGT2B28.[21,46]

A graphical summary of our findings is provided in Figure 8, in which the substrates enzymatic transformations are depicted as well as the transporters involved in their handling and the blockers responsible for inhibitions. Overall, Hoechst33342, GS-MF, and calcein are retained in the presence of KO143, MK571, and PSC833, showing clearly the redundancy between the transporters. Noteworthy is the fact that both KO143 and MK571 can block BCRP, P-gp, and MRPs, although PSC833 appears to be a potent inhibitor for BCRP and P-gp but not the MRPs. The inhibitor concentrations used in this study were chosen on the basis of the concentration where maximum substrate retention was achieved by the model inhibitors in ciPTEC, with no toxic effects (data not shown). Although higher concentrations may promote lack of specificity, the inhibitors either yield none or little inhibition at lower concentrations. This can be explained by the multiple transporters expressed simultaneously in this cell type and the crossover between inhibitors, requiring higher concentrations to discriminate between the particular transporters. However, inhibitory potencies revealed that, despite crossover, the different trans-

DOI: 10.1021/acs.molpharmaceut.5b00821
Mol. Pharmaceutics 2016, 13, 933−944

porters do maintain different specificities toward the inhibitors. Previous reports showed that the presence and activity of transport systems *in vitro* can be assessed with a similar approach and that immortalized cells with poorly retained proximal tubule phenotype, such as HK-2 cells, yield low fluorescent functional properties.[25,29]

After comparing the results obtained in our cell assay with the membrane vesicles assay, the redundancy in substrate and inhibitor specificities could be confirmed. Vesicular transport assays are widely employed for drug screening because they lack complex physiological processes, such as enzyme activity and post-translational regulation, hence, providing an accurate indication of substrate and inhibitor interaction. Our results demonstrated that KO143 and MK571 inhibited BCRP- and MRP4-mediated transport, and PSC833 only inhibited BCRP. On the other hand, the interaction of Hoechst33342 with BCRP and MRP4 could not be identified using the vesicular system. This may be due to the low affinity of Hoechst33342 for BCRP in comparison with E1S, which has a high affinity for the transporter.[38] Note that the concentration used for Hoechst33342 was low and the same as that used for the cellular assays. Furthermore, under these experimental conditions, it was not possible to determine the interaction between the compounds and P-gp in membrane vesicles. This is most likely due to the lipophilicity of the substrates because we used cell-permeable probes. It was recently reported that P-gp activity measurements in vesicular transport assays is jeopardized by the lipophilicity of substrates.[47] Therefore, these substrates require cellular assays, for which overexpression models are well-suited to study a particular transporter in its subcellular environment. Additionally, MDCKII−BCRP/-P-gp cell lines express the enzymes that allowed us to use CMFDA and calcein-AM as substrate. Still, the overexpression systems lack a proper clinical translation[48] as a result of their nonhuman origin and supraphysiological condition. Although the expression of the transporters studied are low in ciPTEC relative to human kidney (Table 1), the relative expression of the transporters is comparable, where MRP4 has the highest expression, followed by P-gp and then BCRP.

Receptor-mediated endocytosis is important for the function of proximal tubular cells, and a deficiency in protein reabsorption will lead to loss of nutrients, proteinuria, inflammation, and renal damage. Drugs, including aminoglycosides, cisplatin, statins, and many others can directly interfere with the different steps of the receptor-mediated endocytosis pathway, for instance, by affecting membrane composition, clathrin availability, dynamin activity, actin skeleton function, vesicle stabilization, or membrane potential.[49] It has been described that cisplatin can affect receptor-mediated endocytosis by inhibiting vacuolar H-ATPase; additionally, statins have been found to inhibit fluorescent protein uptake in opossum kidney cells, but the mechanism remains unclear.[50,51] Also, in inherited diseases such as Dent's disease or nephropathic cystinosis, defects in protein reabsorption can lead to proteinurea and subsequent kidney damage.[52] Furthermore, some compounds are taken up in high concentrations by the proximal tubular cells through receptor-mediated endocytosis and result in nephrotoxicity. Aminoglycosides, such as gentamicin and amikacin, bind the megalin receptor with high affinity and accumulate in the proximal tubule cells.[53] To evaluate protein reabsorption by the proximal tubular cells, we visualized the uptake of proteins in vesicles and compared the cell surface binding on ice with active RAP-GST uptake over time. This 96-well system provides a fast and reproducible approach to measure receptor-mediated endocytosis and can be used to show reduced uptake in patient cells.

Renal models are widely used to study renal clearance and physiology. Although animal studies are often indispensable for providing insight into the clinical relevance of preclinical observations, they are not as easily controlled and are hampered by ethical concerns. Interspecies variability and extrarenal influences, such as body temperature, hormone levels, nervous regulation, hemodynamics, and GFR, can complicate data interpretation even further. By making use of human cell models, many of these factors can be overruled, enabling the study of very specific processes in a fast or high throughput fashion. As a proximal tubule cell model, ciPTEC has proven to be a robust model with its epithelial characteristics, such as basolateral-to-apical polarization, tight-junction formation, and the presence of physiologically relevant enzymatic and transporter activities. Previous findings from our group demonstrated interactions of transporters with endogenous metabolites, sometimes leading to toxicity.[22] This underscores the ability to use ciPTEC in unravelling renal physiology and clearance processes, as well as studying mechanisms leading to renal toxicity. A limitation of our system is that it will only be representative of processes associated with the renal proximal tubules. Drug interactions and drug-induced kidney injury may also be a result of damage to other segments and cellular components of the kidney. However, no representative human cell models of these segments are currently available. Nevertheless, recent advances in the generation of complex human *in vitro* models from renal cell lineages[54] and nephron organoids from induced pluripotent stem cells (hiPS)[55−57] are promising. The importance of validating such models and exploring their potential as predictive tools are key issues that need to be addressed. In addition, recent developments in tissue culture systems acknowledge the importance of the tissue microenvironment in optimal functioning and responsiveness. This can be addressed by culturing cells in a dynamic, 3D environment, allowing optimal communication between cells. Nephron organoids present such 3D environment, as well as PTEC cultured in microfluidic systems[58] (viz., kidney-on-a-chip) or bioartificial tubules.[59] These models are also compatible with high-resolution and real-time molecular imaging, advancing drug interaction studies and their related intracellular effects when applied with suitable fluorescent probes. Our present work describes a set of tools that could be implemented in such a platform and allows studying transport mechanisms that are central to drug absorption, disposition, and detoxification.

In conclusion, we describe an approach that overcomes different limitations of widely used *in vitro* models, namely, vesicles and overexpression cell lines, in order to obtain a more physiological picture of transport systems at the proximal tubule apical membrane. Fluorescent probes are central to this work because they are easy to handle and data acquisition is straightforward and allows the generation, validation, and duplication of functional transport data. Additionally, fluorescent probes are also useful because we prove that, when chosen wisely, a combination of probes and inhibitors can by itself shed light on complex transport mechanisms.

AUTHOR INFORMATION

Corresponding Author

*E-mail: r.masereeuw@uu.nl. Phone: +31(0)30 253 3529. Mobile: +31(0)6-14150261. Fax: +31(0)30 253 7900.

DOI: 10.1021/acs.molpharmaceut.5b00821
Mol. Pharmaceutics 2016, 13, 933−944

Notes

The authors declare no competing financial interest.

■ ACKNOWLEDGMENTS

This work was support by the NephroTools Consortium under the scope of EU FP7Marie Curie actions (grant no. 289754), a grant from the Dutch Kidney Foundation (grant no. KJPB 11.023), as well as The Netherlands Organization for Scientific Research (Zon-MW, grant no. 40-42900-98-2002) The membrane vesicles were kindly provided by Dr. Jan Koenderink and Jeroen van den Heuvel (www.pharmtox.nl).

■ REFERENCES

(1) Varma, M. V.; Feng, B.; Obach, R. S.; Troutman, M. D.; Chupka, J.; Miller, H. R.; et al. Physicochemical determinants of human renal clearance. *J. Med. Chem.* **2009**, *52* (15), 4844−52.

(2) Masereeuw, R.; Russel, F. G. Regulatory pathways for ATP-binding cassette transport proteins in kidney proximal tubules. *AAPS J.* **2012**, *14* (4), 883−94.

(3) Mutsaers, H. A.; van den Heuvel, L. P.; Ringens, L. H.; Dankers, A. C.; Russel, F. G.; Wetzels, J. F.; et al. Uremic toxins inhibit transport by breast cancer resistance protein and multidrug resistance protein 4 at clinically relevant concentrations. *PLoS One* **2011**, *6* (4), e18438.

(4) Pavek, P.; Merino, G.; Wagenaar, E.; Bolscher, E.; Novotna, M.; Jonker, J. W.; Schinkel, A. H. Human breast cancer resistance protein: interactions with steroid drugs, hormones, the dietary carcinogen 2-amino-1-methyl-6-phenylimidazo(4,5-b)pyridine, and transport of cimetidine. *J. Pharmacol Exp Ther.* **2005**, *312* (1), 144−152.

(5) Leslie, EM; Deeley, RG; Cole, SP. Multidrug resistance proteins: role of P-glycoprotein, MRP1, MRP2, and BCRP (ABCG2) in tissue defense. *Toxicol Appl Pharmacol.* **2005**, *204* (3), 216−237.

(6) Giacomini, K. M.; Huang, S. M.; Tweedie, D. J.; Benet, L. Z.; Brouwer, K. L.; et al. Membrane transporters in drug development. *Nat. Rev. Drug Discovery* **2010**, *9* (3), 215−236.

(7) Perazella, M. A. Drug-induced renal failure: update on new medications and unique mechanisms of nephrotoxicity. *Am. J. Med. Sci.* **2003**, *325* (6), 349−62.

(8) Kitterer, D.; Schwab, M.; Alscher, M. D.; Braun, N.; Latus, J. Drug-induced acid-base disorders. *Pediatr. Nephrol.* **2015**, *30*, 1407.

(9) Christensen, E. I.; Birn, H.; Storm, T.; Weyer, K.; Nielsen, R. Endocytic receptors in the renal proximal tubule. *Physiology* **2012**, *27* (4), 223−36.

(10) Wagner, M. C.; Campos-Bilderback, S. B.; Chowdhury, M.; Flores, B.; Lai, X.; Myslinski, J.; et al. Proximal Tubules Have the Capacity to Regulate Uptake of Albumin. *J. Am. Soc. Nephrol.* **2016**, *27*, 482.

(11) Abbate, M.; Zoja, C.; Remuzzi, G. How does proteinuria cause progressive renal damage? *J. Am. Soc. Nephrol.* **2006**, *17* (11), 2974−84.

(12) Gorriz, J. L.; Martinez-Castelao, A. Proteinuria: detection and role in native renal disease progression. *Transplant Rev-Orlan.* **2012**, *26* (1), 3−13.

(13) Karlsson, J. E.; Heddle, C.; Rozkov, A.; Rotticci-Mulder, J.; Tuvesson, O.; Hilgendorf, C.; et al. High-activity p-glycoprotein, multidrug resistance protein 2, and breast cancer resistance protein membrane vesicles prepared from transiently transfected human embryonic kidney 293-epstein-barr virus nuclear antigen cells. *Drug Metab. Dispos.* **2010**, *38* (4), 705−14.

(14) El-Sheikh, A. A.; Greupink, R.; Wortelboer, H. M.; van den Heuvel, J. J.; Schreurs, M.; Koenderink, J. B.; et al. Interaction of immunosuppressive drugs with human organic anion transporter (OAT) 1 and OAT3, and multidrug resistance-associated protein (MRP) 2 and MRP4. *Transl Res.* **2013**, *162* (6), 398−409.

(15) Wittgen, H. G.; van den Heuvel, J. J.; van den Broek, P. H.; Dinter-Heidorn, H.; Koenderink, J. B.; Russel, F. G. Cannabinoid type 1 receptor antagonists modulate transport activity of multidrug resistance-associated proteins MRP1, MRP2, MRP3, and MRP4. *Drug Metab. Dispos.* **2011**, *39* (7), 1294−1302.

(16) Gartzke, D.; Fricker, G. Establishment of optimized MDCK cell lines for reliable efflux transport studies. *J. Pharm. Sci.* **2014**, *103* (4), 1298−304.

(17) Konig, J.; Muller, F.; Fromm, M. F. Transporters and drug-drug interactions: important determinants of drug disposition and effects. *Pharmacol. Rev.* **2013**, *65* (3), 944−66.

(18) Fahrmayr, C.; Konig, J.; Auge, D.; Mieth, M.; Munch, K.; Segrestaa, J.; et al. Phase I and II metabolism and MRP2-mediated export of bosentan in a MDCKII-OATP1B1-CYP3A4-UGT1A1-MRP2 quadruple-transfected cell line. *British journal of pharmacology* **2013**, *169* (1), 21−33.

(19) Nagai, J.; Sato, K.; Yumoto, R.; Takano, M. Megalin/cubilin-mediated uptake of FITC-labeled IgG by OK kidney epithelial cells. *Drug Metab. Pharmacokinet.* **2011**, *26* (5), 474−85.

(20) Vegt, E.; van Eerd, J. E.; Eek, A.; Oyen, W. J.; Wetzels, J. F.; de Jong, M.; et al. Reducing renal uptake of radiolabeled peptides using albumin fragments. *J. Nucl. Med.* **2008**, *49* (9), 1506−11.

(21) Mutsaers, H. A.; Wilmer, M. J.; Reijnders, D.; Jansen, J.; van den Broek, P. H.; Forkink, M.; et al. Uremic toxins inhibit renal metabolic capacity through interference with glucuronidation and mitochondrial respiration. *Biochim. Biophys. Acta, Mol. Basis Dis.* **2013**, *1832* (1), 142−50.

(22) Schophuizen, C. M.; Wilmer, M. J.; Jansen, J.; Gustavsson, L.; Hilgendorf, C.; Hoenderop, J. G.; et al. Cationic uremic toxins affect human renal proximal tubule cell functioning through interaction with the organic cation transporter. *Pfluegers Arch.* **2013**, *465* (12), 1701−14.

(23) Wilmer, M. J.; Saleem, M. A.; Masereeuw, R.; Ni, L.; van der Velden, T. J.; Russel, F. G.; et al. Novel conditionally immortalized human proximal tubule cell line expressing functional influx and efflux transporters. *Cell Tissue Res.* **2010**, *339* (2), 449−57.

(24) Gorvin, C. M.; Wilmer, M. J.; Piret, S. E.; Harding, B.; van den Heuvel, L. P.; Wrong, O.; et al. Receptor-mediated endocytosis and endosomal acidification is impaired in proximal tubule epithelial cells of Dent disease patients. *Proc. Natl. Acad. Sci. U. S. A.* **2013**, *110* (17), 7014−9.

(25) Bircsak, K. M.; Gibson, C. J.; Robey, R. W.; Aleksunes, L. M. Assessment of drug transporter function using fluorescent cell imaging. *Curr. Protoc Toxicol.* **2013**, *57*, 1−23.

(26) Mahringer, A.; Delzer, J.; Fricker, G. A fluorescence-based in vitro assay for drug interactions with breast cancer resistance protein (BCRP, ABCG2). *Eur. J. Pharm. Biopharm.* **2009**, *72* (3), 605−13.

(27) Weiss, J.; Theile, D.; Ketabi-Kiyanvash, N.; Lindenmaier, H.; Haefeli, W. E. Inhibition of MRP1/ABCC1, MRP2/ABCC2, and MRP3/ABCC3 by nucleoside, nucleotide, and non-nucleoside reverse transcriptase inhibitors. *Drug Metab. Dispos.* **2007**, *35* (3), 340−344.

(28) Luna-Tortos, C.; Fedrowitz, M.; Loscher, W. Evaluation of transport of common antiepileptic drugs by human multidrug resistance-associated proteins (MRP1, 2 and 5) that are overexpressed in pharmacoresistant epilepsy. *Neuropharmacology* **2010**, *58* (7), 1019−32.

(29) Jenkinson, S. E.; Chung, G. W.; van Loon, E.; Bakar, N. S.; Dalzell, A. M.; Brown, C. D. The limitations of renal epithelial cell line HK-2 as a model of drug transporter expression and function in the proximal tubule. *Pfluegers Arch.* **2012**, *464* (6), 601−11.

(30) Ivanova, E. A.; De Leo, M. G.; Van Den Heuvel, L.; Pastore, A.; Dijkman, H.; De Matteis, M. A.; et al. Endo-lysosomal dysfunction in human proximal tubular epithelial cells deficient for lysosomal cystine transporter cystinosin. *PLoS One* **2015**, *10* (3), e0120998.

(31) Vicinanza, M.; Di Campli, A.; Polishchuk, E.; Santoro, M.; Di Tullio, G.; Godi, A.; et al. OCRL controls trafficking through early endosomes via PtdIns4,5P(2)-dependent regulation of endosomal actin. *EMBO J.* **2011**, *30* (24), 4970−85.

(32) Bu, G. J.; Geuze, H. J.; Strous, G. J.; Schwartz, A. L. 39-Kda Receptor-Associated Protein Is an Er Resident Protein and Molecular Chaperone for Ldl Receptor-Related Protein. *EMBO J.* **1995**, *14* (10), 2269−2280.

(33) Jansen, J.; Schophuizen, C. M.; Wilmer, M. J.; Lahham, S. H.; Mutsaers, H. A.; Wetzels, J. F.; et al. A morphological and functional

DOI: 10.1021/acs.molpharmaceut.5b00821
Mol. Pharmaceutics 2016, 13, 933−944

comparison of proximal tubule cell lines established from human urine and kidney tissue. *Exp. Cell Res.* **2014**, *323* (1), 87−99.
(34) Jonker, J. W.; Smit, J. W.; Brinkhuis, R. F.; Maliepaard, M.; Beijnen, J. H.; Schellens, J. H. M.; Schinkel, A. H. Role of breast cancer resistance protein in the bioavailability and fetal penetration of topotecan. *J. Natl. Cancer I.* **2000**, *92* (20), 1651−1656.
(35) Pastan, I.; Gottesman, M. M.; Ueda, K.; Lovelace, E.; Rutherford, A. V.; Willingham, M. C. A Retrovirus Carrying an Mdr1 Cdna Confers Multidrug Resistance and Polarized Expression of P-Glycoprotein in Mdck Cells. *Proc. Natl. Acad. Sci. U. S. A.* **1988**, *85* (12), 4486−90.
(36) El-Sheikh, A. A.; van den Heuvel, J. J.; Koenderink, J. B.; Russel, F. G. Interaction of nonsteroidal anti-inflammatory drugs with multidrug resistance protein (MRP) 2/ABCC2- and MRP4/ABCC4-mediated methotrexate transport. *J. Pharmacol. Exp. Ther.* **2007**, *320* (1), 229−235.
(37) Wittgen, H. G.; van den Heuvel, J. J.; van den Broek, P. H.; Siissalo, S.; Groothuis, G. M.; de Graaf, I. A.; et al. Transport of the coumarin metabolite 7-hydroxycoumarin glucuronide is mediated via multidrug resistance-associated proteins 3 and 4. *Drug Metab. Dispos.* **2012**, *40* (6), 1076−9.
(38) Dankers, A. C.; Sweep, F. C.; Pertijs, J. C.; Verweij, V.; van den Heuvel, J. J.; Koenderink, J. B.; et al. Localization of breast cancer resistance protein (Bcrp) in endocrine organs and inhibition of its transport activity by steroid hormones. *Cell Tissue Res.* **2012**, *349* (2), 551−63.
(39) Thomas, P.; Smart, T. G. HEK293 cell line: a vehicle for the expression of recombinant proteins. *J. Pharmacol. Toxicol. Methods* **2005**, *51* (3), 187−200.
(40) Shukla, S.; Schwartz, C.; Kapoor, K.; Kouanda, A.; Ambudkar, S. V. Use of baculovirus BacMam vectors for expression of ABC drug transporters in mammalian cells. *Drug Metab. Dispos.* **2012**, *40* (2), 304−12.
(41) Van Aubel, R. A.; Koenderink, J. B.; Peters, J. G.; Van Os, C. H.; Russel, F. G. Mechanisms and interaction of vinblastine and reduced glutathione transport in membrane vesicles by the rabbit multidrug resistance protein Mrp2 expressed in insect cells. *Mol. Pharmacol.* **1999**, *56* (4), 714−719.
(42) Muenster, U.; Grieshop, B.; Ickenroth, K.; Gnoth, M. J. Characterization of substrates and inhibitors for the in vitro assessment of Bcrp mediated drug-drug interactions. *Pharm. Res.* **2008**, *25* (10), 2320−6.
(43) Videmann, B.; Tep, J.; Cavret, S.; Lecoeur, S. Epithelial transport of deoxynivalenol: involvement of human P-glycoprotein (ABCB1) and multidrug resistance-associated protein 2 (ABCC2). *Food Chem. Toxicol.* **2007**, *45* (10), 1938−47.
(44) Gozalpour, E.; Greupink, R.; Bilos, A.; Verweij, V.; van den Heuvel, J. J.; Masereeuw, R.; et al. Convallatoxin: a new P-glycoprotein substrate. *Eur. J. Pharmacol.* **2014**, *744*, 18−27.
(45) Fardel, O.; Le Vee, M.; Jouan, E.; Denizot, C.; Parmentier, Y. Nature and uses of fluorescent dyes for drug transporter studies. *Expert Opin. Drug Metab. Toxicol.* **2015**, *11* (8), 1233−51.
(46) Huls, M.; Brown, C. D.; Windass, A. S.; Sayer, R.; van den Heuvel, J. J.; Heemskerk, S.; et al. The breast cancer resistance protein transporter ABCG2 is expressed in the human kidney proximal tubule apical membrane. *Kidney Int.* **2008**, *73* (2), 220−5.
(47) Gozalpour, E.; Wittgen, H. G.; van den Heuvel, J. J.; Greupink, R.; Russel, F. G.; Koenderink, J. B. Interaction of digitalis-like compounds with p-glycoprotein. *Toxicol. Sci.* **2013**, *131* (2), 502−11.
(48) Pan, C.; Kumar, C.; Bohl, S.; Klingmueller, U.; Mann, M. Comparative proteomic phenotyping of cell lines and primary cells to assess preservation of cell type-specific functions. *Mol. Cell. Proteomics* **2009**, *8* (3), 443−50.
(49) Dutta, D.; Donaldson, J. G. Search for inhibitors of endocytosis: Intended specificity and unintended consequences. *Cell Logist.* **2012**, *2* (4), 203−8.
(50) Takano, M.; Nakanishi, N.; Kitahara, Y.; Sasaki, Y.; Murakami, T.; Nagai, J. Cisplatin-induced inhibition of receptor-mediated endocytosis of protein in the kidney. *Kidney Int.* **2002**, *62* (5), 1707−17.
(51) Sidaway, J. E.; Davidson, R. G.; McTaggart, F.; Orton, T. C.; Scott, R. C.; Smith, G. J.; Brunskill, N. J. Inhibitors of 3-hydroxy-3-methylglutaryl-CoA reductase reduce receptor-mediated endocytosis in opossum kidney cells. *J. Am. Soc. Nephrol.* **2004**, *15* (9), 2258−2265.
(52) Wilmer, M. J.; Emma, F.; Levtchenko, E. N. The pathogenesis of cystinosis: mechanisms beyond cystine accumulation. *Am. J. Physiol Renal Physiol.* **2010**, *299* (5), F905−16.
(53) Nagai, J.; Takano, M. Molecular aspects of renal handling of aminoglycosides and strategies for preventing the nephrotoxicity. *Drug Metab. Pharmacokinet.* **2004**, *19* (3), 159−70.
(54) Lam, A. Q.; Freedman, B. S.; Bonventre, J. V. Directed differentiation of pluripotent stem cells to kidney cells. *Semin. Nephrol.* **2014**, *34* (4), 445−61.
(55) Xia, Y.; Sancho-Martinez, I.; Nivet, E.; Rodriguez Esteban, C.; Campistol, J. M.; Izpisua Belmonte, J. C. The generation of kidney organoids by differentiation of human pluripotent cells to ureteric bud progenitor-like cells. *Nat. Protoc.* **2014**, *9* (11), 2693−704.
(56) Takasato, M.; Er, P. X.; Chiu, H. S.; Maier, B.; Baillie, G. J.; Ferguson, C.; et al. Kidney organoids from human iPS cells contain multiple lineages and model human nephrogenesis. *Nature* **2015**, *526* (7574), 564−8.
(57) Morizane, R.; Lam, A. Q.; Freedman, B. S.; Kishi, S.; Valerius, M. T.; Bonventre, J. V. Nephron organoids derived from human pluripotent stem cells model kidney development and injury. *Nat. Biotechnol.* **2015**, *33*, 1193.
(58) Jang, K. J.; Mehr, A. P.; Hamilton, G. A.; McPartlin, L. A.; Chung, S.; Suh, K. Y.; et al. Human kidney proximal tubule-on-a-chip for drug transport and nephrotoxicity assessment. *Integr Biol. (Camb).* **2013**, *5* (9), 1119−29.
(59) Jansen, J.; De Napoli, I. E.; Fedecostante, M.; Schophuizen, C. M.; Chevtchik, N. V.; Wilmer, M. J.; et al. Human proximal tubule epithelial cells cultured on hollow fibers: living membranes that actively transport organic cations. *Sci. Rep.* **2015**, *5*, 16702.

DOI: 10.1021/acs.molpharmaceut.5b00821
Mol. Pharmaceutics 2016, 13, 933−944